EXPERIMENTAL INVESTIGATION OF SPECIFIC HEAT OF AQUEOUS GRAPHENE OXIDE Al_2O_3 HYBRID NANOFLUID

by

Yuguo GAO [a,b*], ***Yangyang XI*** [a], ***Zhenzhong YANG*** [a*], ***Agus P. SASMITO*** [b*], ***Arun S. MUJUMDAR*** [b,c], ***and Lijun WANG*** [a]

[a] School of Mechanical Engineering,
North China University of Water Resources and Electric Power,
Zhengzhou, Henan Province, China
[b] McGill University, Department of Mining and Materials Engineering,
Montreal, Canada
[c] University of Western Ontario, Department Chemical and Biochemical Engineering,
Thompson Engineering Building, London, Canada

Original scientific paper
https://doi.org/10.2298/TSCI190404381G

The specific heat of aqueous graphene+Al_2O_3 (1:1) hybrid nanofluid was measured using the cooling method. The influence of nanoparticle mass fraction and temperature on the specific heat capacity of the hybrid nanofluids was investigated, the specific heat of the hybrid nanofluid was compared with that of aqueous graphene oxide nanofluid and Al_2O_3 nanofluid. A fitted formula of the specific heat of the hybrid nanofluid was proposed based on the experimental data. It indicates that the specific heat reduction ratio increases with increase of nanoparticle fraction and the maximum reduction ratio is 7% at 0.15 wt.% at 20 °C. The mass fraction of nanoparticle affects the specific heat of hybrid nanofluid more significantly at lower temperature. Temperature impacts the specific heat more distinctly than the nanoparticle fraction. The specific heat increases with temperature and the maximum specific heat reduction ratio of the hybrid nanofluid diminishes from 7% at 20 °C to 2% at 70 °C at the mass fraction of 0.05%.

Key words: *hybrid nanofluid, graphene oxide, Al_2O_3, specific heat capacity, experiment*

Introduction

Nanofluids have a wide range of applications [1, 2]. It is a solid-liquid two-phase mixture formed by suspending nanosized particles (less than 100 nm) in a liquid. The nanofluids have unique heat transfer characteristics. They have significantly improved thermal conductivity, providing enhanced heat transfer performance with less abrasion or pipe blockage compared to a macro-particle two phase fluids [3-9]. They also play a very important role in PCM, such as enhancing specific heat capacity [10], reducing supercooling degree, and increasing thermal conductivity [11].

Nanofluids can be divided into two categories according to the types of nanoparticles. First is a single nanofluid formed by a single nanoparticle and base liquids, the other is a hybrid nanofluid formed by mixing multiple nanoparticles and base liquids. The deficiency with single nanofluids is that they either have good thermal networks or have better rheologi-

* Corresponding author, e-mail: gaoyuguo@ncwu.edu.cn, yzzho@163.com, agus.sasmito@mcgill.ca,

cal properties, but not all the features that are necessary for a particular application. Thus, there is a trade-off between the characteristics, which leads to a number of limitations in single particle type nanofluids for practical applications. Hybrid nanofluids have better thermal network and rheological properties simultaneously, which can make up for the limitations of single nanofluids in applications [12]. However, research is relatively scarce in the preparation, determination of thermal properties, as well as heat transfer and friction factor of hybrid nanofluids [13]. In addition, there were many studies performed to characterize the thermal conductivity of nanofluids [9, 14], but fewer on the specific heat capacity of nanofluids. Moreover, most of the existing studies that focus on the specific heat capacity of single-nanoparticle nanofluids [15-18], even fewer on that of hybrid nanofluids. As a very important thermophysical parameter, specific heat also has crucial influence on the temperature field, heat transfer and thermal energy storage directly [19, 20].

Yarmand *et al.* [15] measured the specific heat of graphene/platinum hybrid nanofluids. They observed that the specific heat of the hybrid nanofluid decreases with the increase of nanoparticle concentration. The specific heat capacity of a hybrid nanofluid of mass fraction 0.02 wt.%, 0.1 wt.% is about 1.77% and 6.26% lower than that of the base fluid at 45 °C, respectively. Saeedinia *et al.* [16] studied the specific heat capacity of oil-based CuO nanofluids with 0.2-2 wt.% at different temperatures. Their results show that the specific heat capacity of the nanofluid is lower than that of the base fluid, and decreases with increase of nanoparticle concentration. Nieh *et al.* [21] used Al_2O_3 and TiO_2 nanocoolant to improve the heat dissipation performance of an air-cooled radiator. They found the specific heat of the nanocoolant gradually decreases with the increase of the concentration of Al_2O_3 and TiO_2 due to the low specific heat of Al_2O_3 and TiO_2 nanoparticles. Vajjha and Das [22] determined the specific heat of the fluid by dispersing Al_2O_3, ZnO nanoparticles in propylene glycol-water (volume ratio 60:40). They found the specific heat decreases with the increase of volume concentration of nanoparticles and increases with the increase of temperature. Ho *et al.* [23] studied the effect of dispersed nanoparticles on the thermal properties of aqueous PCM suspension. It was found that dispersing Al_2O_3 nanoparticles in the PCM suspension reduces the effective specific heat of the hybrid suspension significantly, especially in the absence of a phase change in the microencapsulated phase change material (MEPCM) particles. Hu *et al.* [24] investigated the effective specific heat capacity of PCM, binary nitrate eutectic with silica nanoparticles used in concentrating solar power plants, using both experimental measurements and molecular dynamics simulations. The results showed the specific heat capacity increases when adding 10 nm silica nanoparticles up to 1.0 wt.%, and then it decreases at higher concentrations. The 20 nm nanoparticles display a maximum enhancement in the average specific heat capacity (by ~26.7%). The molecular dynamics simulation indicated that the change of Coulombic energy contributes the most to the variation of specific heat capacity.

Ice slurry, a useful aqueous PCM at the cold side of the heat engine, is an excellent way of storing energy even in large quantities [25]. Liu *et al.* [26-28] studied the nucleation rate and supercooling degree of ice slurry. They found graphene oxide (GO) nanofluids can be used as alternative PCM in cold storage application because of their low supercooling degrees. The supercooling degrees were reduced by more than 74% with the increase in volume concentration of GO. The addition of oxygen-containing functional groups on GO makes it more active than graphene and can also improve its properties through various reactions with oxygen-containing functional groups.

Furthermore, GO is hydrophilic and has a superior dispersion stability and higher thermal conductivity [29, 30]. Nano Al_2O_3 is a common metal oxide material and is widely used in various nanofluids because the Al_2O_3 nanofluid has lower viscosity and better rheological behavior as compared to other particles such as copper oxide [31, 32]. It offers obvious advantages such as higher thermal conductivity, cheap, safe, good stability in water [33-36]. Nevertheless, research on the specific heat of hybrid nanofluids formed by Al_2O_3, GO and water has not been reported. This study is motivated by the potential advantages of these two nanomaterials to prepare a new hybrid nanofluid for using as ice slurry, *i. e.* using nano Al_2O_3 and GO as the dispersed phase and deionized water as the base fluid. The specific heat of the hybrid nanofluid will be determined to consider its influence on performance of the ice slurry.

There are many methods to determine specific heat capacity [37]. The widespread ways are calorimetric measurements [38-42] and law of cooling [43-46]. As a more accurate and convenient method, the *cooling method* is employed to measure the specific heat of the hybrid nanofluids at various temperatures and nanoparticle mass fractions. Moreover, a fitted formula of specific heat capacity for the hybrid nanofluid is proposed based on the experimental results.

Experimental procedure

Preparation and characterization of hybrid nanofluid

The hybrid nanofluids were prepared by the well-known two-step method. The GO (purity ≥ 99 wt.%, layer number < 10, Shenzhen Turing Evolution Technology Co., Ltd.), aluminum oxide nanoparticles (purity ≥ 99.99%, average particle size of 30 ± 5 nm, Shanghai Maikun Chemical Co., LTD), and sodium dodecyl sulfate (SDS) dispersant (anion, analytical purity, Beijing Biotechnology Co., Ltd.) were added to deionized water to form hybrid nanofluids of different mass fractions, and the pH was determined by acidity meter. After stirring for 30 minutes with a magnetic stirrer, it was sonicated for 90 minutes to obtain a uniformly dispersed stable nanofluid. The change of the nanofluid stability was tested by WGZ-2000 Turbidimeter (Shanghai Xin Rui Instrument Co. Ltd.). The 4 mL of the hybrid nanofluid was extracted from the upper section of the container and was diluted by three times with deionized water. The absorbance of the hybrid nanofluids was measured with time using the turbidimeter. The absorbance reduction ratio (ARR) is defined as:

$$ARR\% = \frac{A_0 - A_n}{A_0}100 \qquad (1)$$

where A_0 and A_n are initial absorbance and absorbance at time n, respectively.

Figure 1 is the SEM of dispersion of hybrid nanoparticles in the base solution, which shows that the Al_2O_3 nanoparticles disperse in the GO homogenously. Figure 2 shows the influence of SDS mass fraction on the absorbance and the ARR. The absorbance decreases greatly over the first four days and then the decrease slows down, and the ARR is reduced by 30-50% in seven days when adding SDS as dispersant, which shows the dispersant makes the hybrid nanofluid more stable.

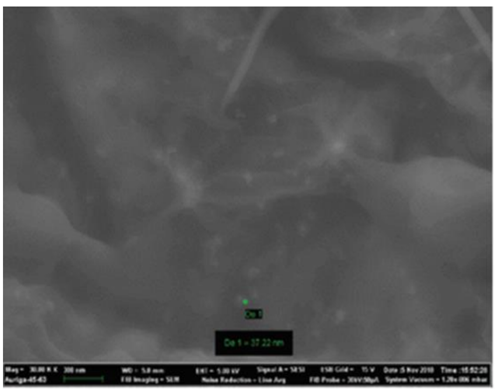

Figure 1. The SEM of dispersion of hybrid nanoparticles in the base solution

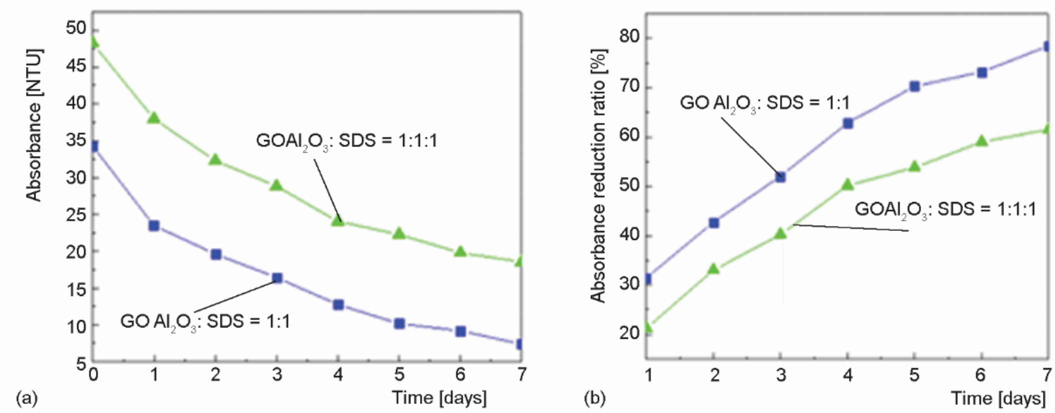

Figure 2. Influence of SDS on absorbance (a) and ARR (b)

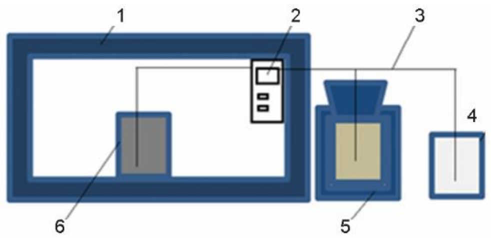

Figure 3. Schematic diagram of test rig;
1 – incubator, 2 – temperature controller and recorder, 3 – temperature sensor connector, 4 – container for lower temperature sample, 5 – adiabatic container, 6 – container for higher temperature sample

Determination of specific heat capacity

The specific heat capacity of the liquid was determined by the cooling method. Figure 3 shows the schematic diagram of the test rig. A. Sample of mass, M_1, was put into a small container of mass, M_c, and specific heat, $Cp_{,c}$, also heated up to the required temperature, T_1, using the incubator in the specific heat capacity instrument (BRR-II/II, Xiangtan Xiangyi instrument Co. LTD, China). It was then transferred to an adiabatic container quickly. The deionized water as standard sample was kept at a lower temperature, T_2. The standard sample of mass, M_2, was quickly poured into the hybrid nanofluid sample and the mixing temperature, T_3, was measured and recorded until the temperature remained constant. The equations express the applicable heat balances:

$$Q_1 = Q_2 + Q_L \tag{2}$$

$$Q_1 = (C_{p,\mathrm{nf}} M_1 + C_{p,c} M_c)(T_1 - T_3) \tag{3}$$

$$Q_2 = C_{p,\mathrm{bf}} M_2 (T_3 - T_2) \tag{4}$$

The Q_1 is the heat released by hybrid nanofluid sample and container Q_2 – the absorbed heat by deionized water, Q_L – the heat loss, $C_{p,\mathrm{nf}}$, $C_{p,\mathrm{bf}}$ are the specific heat capacity of hybrid nanofluid and deionized water, respectively. The mixing system is adiabatic. The temperature of the low temperature sample equates to the environment temperature in the measurement, and the mixing equilibrium time of two fluids is shorter than that between solid and liquid. Therefore, the heat loss from the mixture fluid to the environment is very small and Q_L can be neglected. A small and thin-wall glass container is used, so the released heat by container can also be neglected. Therefore:

$$C_{p,\mathrm{nf}} = \frac{C_{p,\mathrm{bf}} M_2 (T_3 - T_2)}{M_1 (T_1 - T_3)} \tag{5}$$

The temperature probes in the instrument have an accuracy of 0.1 °C, and the accuracy of the electronic balance is 0.1 mg. The measurement is repeated five times for each sample at the same temperature. The experimental uncertainty is calculated according to:

$$\frac{\delta C_{p,\mathrm{nf}}}{\left|C_{p,\mathrm{nf}}\right|} = \sqrt{\left(\frac{\delta T_1}{|T_1|}\right)^2 + \left(\frac{\delta T_2}{|T_2|}\right)^2 + \left(\frac{\delta T_3}{|T_3|}\right)^2 + \left(\frac{\delta M_1}{|M_1|}\right)^2 + \left(\frac{\delta M_2}{|M_2|}\right)^2} \tag{6}$$

The average uncertainty is 1.36% at the range of nanoparticle mass fraction 0.05-0.15 wt.% and temperature 20-70 °C.

Reliability validation

The specific heat capacity of the deionized water was measured to verify the reliability of the experimental system. Figure 4 shows the comparison between the experimental results of deionized water and the standard data in literature [47]. It can be seen that the error is within ±1.4%, which means the experimental system is stable and reliable.

Results and discussion

Influence of nanoparticle mass fraction on the specific heat of hybrid nanofluids

Figure 5 shows the influence of temperature and mass fraction on the specific heat capacity wherein the mass ratio of the Al_2O_3 and GO is 1:1. It reveals the specific heat capacity of the nanofluid decreases with the increase of nanoparticle mass fraction. The specific heat capacity of the 0.05 wt.% and 0.15 wt.% hybrid nanofluid reduces by 4% and 7% as compared to the base liquid at 20 °C, respectively. The specific heat of the 0.05 wt.% hybrid nanofluid reduces by 1% at 70 °C, and the specific heat capacity of the 0.15 wt.% hybrid nanofluid reduces by 0.5% compared to that of the 0.05 wt.% hybrid nanofluid at 70 °C. This

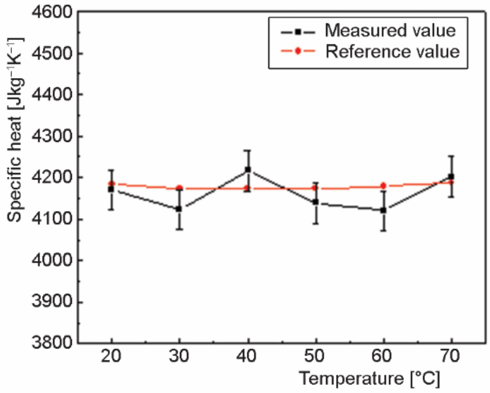

Figure 4. Comparison between experimental results of the specific heat capacity of deionized water and the standard data

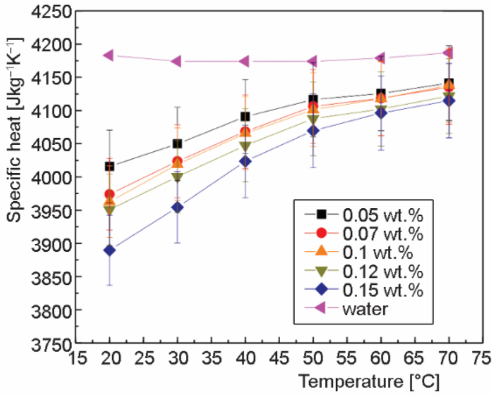

Figure 5. Relations of the specific heat, nanoparticle mass fraction and temperature of the hybrid nanofluid

is due to water having higher specific heat than that of the nanoparticles on one hand, on the other hand, it shows the hybrid nanoparticle affects specific heat capacity heavily, even a small amount of mass fraction nanoparticle can reduce the specific heat capacity greatly, especially at lower temperature.

Figure 6 is the heat capacity reduction ratio of the hybrid nanofluid, which is defined:

$$C_{p_r}\% = \left(\frac{C_{p,\mathrm{bf}} - C_{p,\mathrm{nf}}}{C_{p,\mathrm{bf}}}\right)100 \tag{7}$$

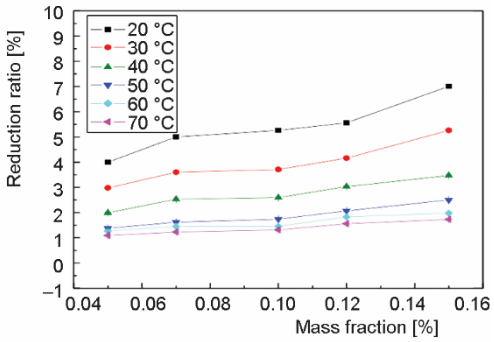

Figure 6. Influence of mass fraction on heat capacity reduction ratio of the hybrid nanofluid

It indicates that the heat capacity reduction ratio increases with the increase of nanoparticle mass fraction, with maximum reduction ratio of almost 7% at 0.15 wt.% at 20 °C, which is about seven times than that at 0.05% at 70 °C. At the same temperature, when mass fraction increases from 0.05 wt.% to 0.15 wt.%, the average reduction ratio increases by 1.5%, which means the mass fraction of nanoparticle affects the specific heat of hybrid nanofluid more significantly at lower temperature.

Influence of temperature on specific heat capacity of hybrid nanofluid

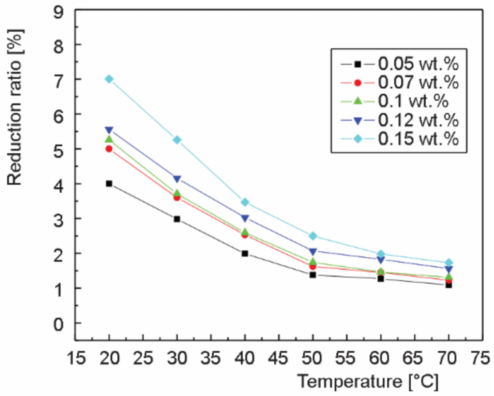

Figure 7. Influence of temperature on specific heat reduction ratio of the hybrid nanofluid

Besides fig. 5, fig. 7 shows distinctly the influence of temperature on the specific heat of the hybrid nanofluid. It can be observed that the specific heat increases with temperature greatly, indicating that the temperature impacts the specific heat more strongly than mass fraction of nanoparticle. The specific heat reduction ratio of the 0.05 wt.% hybrid nanofluid decreases from 4% at 20 °C to 1% at 70 °C, respectively, displaying amplitude drop of up to four times. Similarly, the specific heat reduction ratio of 0.15 wt.% hybrid nanofluid diminishes from 7% at 20 °C to 2% at 70 °C, *i. e.* drop amplitude of 3.5 times. This is mainly due to the fact that nanoparticles change the microstructure of the base liquid [24], and the micro-motion of the nanoparticles is greatly enhanced at a higher temperature, thereby improving the internal energy of the hybrid nanofluid.

Comparison of specific heat between single nanoparticle and hybrid nanofluids

Figure 8 contrasts the specific heats of the hybrid and the single nanoparticle nanofluids, GO-water nanofluid and Al_2O_3-water nanofluid, with the same mass fraction nanoparticles of 0.1%. It indicates all specific heat capacities increase with temperature. The hybrid nanofluid has the highest specific heat after water. However, the differences among the specific heat of nanofluids are not large, maximum difference of 1.33% at 20 °C. This is due to the specific heat capacity of the GO being close to that of the alumina nanoparticle, and the fact that the concentration of the nanofluid is very dilute.

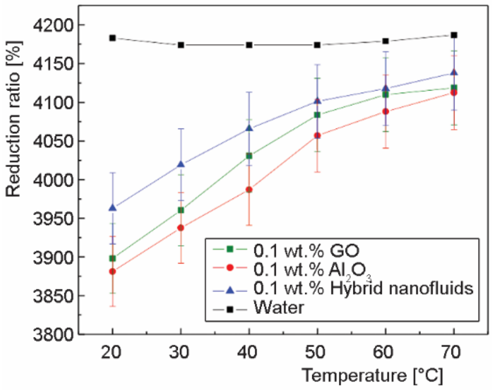

Figure 8. Specific heat of single nanoparticle and hybrid nanofluids

Experimental fitting of the specific heat of hybrid nanofluid

The microscopic state of the base fluid is disrupted when the nanoparticle is dispersed into it. For nanoparticles, the free surface of the nanoparticle turns into a non-free surface due to the binding of liquid molecules [48]. The surface free energy accounts for a large proportion of the system energy due to the large specific surface area, which will greatly affect the specific heat capacity of the nanofluid. Moreover, the structure of the liquid also changes with the addition of the nanoparticles [24], and a part of liquid molecules are coated on the surface of the nanoparticles to form a liquid layer in which the arrangement of the liquid molecule changes, and the free energy state is changed. There are currently mathematical models based on classical mixing theory for calculating the specific heat of hybrid nanofluids. One was proposed by Ho *et al.* [23] as:

$$\rho_{\rm nf}C_{p,\rm nf} = \varphi_{\rm np1}\rho_{\rm np1}C_{p,\rm np1} + \varphi_{\rm np2}\rho_{\rm np2}C_{p,\rm np2} + (1-\varphi_{\rm np1}-\varphi_{\rm np2})\rho_{\rm bf}C_{p,\rm bf} \tag{8}$$

where subscripts np1 and np2 are two kinds of nanoparticles, φ – the volume fraction, and ρ [kgm^{-3}] – the density.

Sundar *et al.* [49] used the following equations

$$C_{p,\rm np} = \frac{(C_{p,\rm np1})w_{\rm np1} + (C_{p,\rm np2})w_{\rm np2}}{w_{\rm np1} + w_{\rm np2}} \tag{9}$$

$$C_{p,\rm nf} = \varphi C_{p,\rm np} + (1-\varphi)C_{p,\rm bf} \tag{10}$$

where w is the mass fraction. The relation between mass fraction and volume fraction is given [48]:

$$\varphi = \frac{w\rho_{\rm bf}}{w\rho_{\rm bf} + \rho_{\rm np}(1-w)} \tag{11}$$

The specific heat capacity of GO is approximately equal to that of graphene 790 J/kgK [50], the density of GO is 2.63 g/cm^3, the specific heat capacity of alumina is 773 J/kgK, and the density of alumina is 3.6 g/cm^3 [51]. The calculated values according to eqs. (8) and (10) and the experimental values at 30 ° C were compared in fig. 9. It can be seen that the results predicted by the two models are almost identical and are larger than the experimental data, with maximum error of 11.2%. This is because the two models only consider the influence of density and mass fraction on the heat, but do not consider other factors such as the effect of temperature on the specific heat of the hybrid nanofluid.

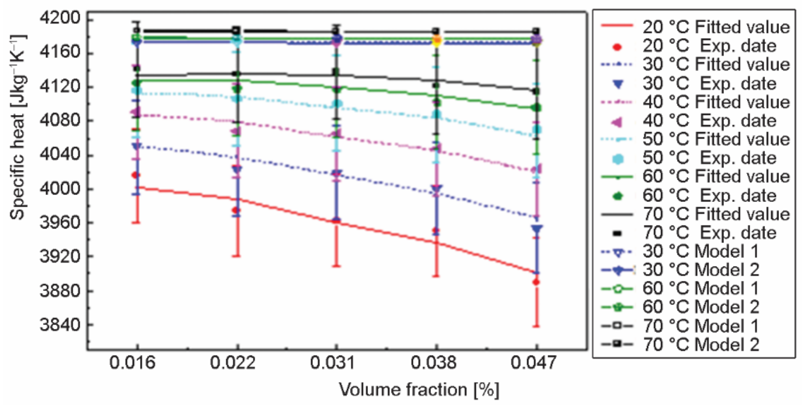

Figure 9. Comparison between predicted values of models and experimental data
(*for color image see journal web site*)

It is known from the experiment that the temperature impacts the specific heat greatly. Thus, a new equation, fitted by the experimental data, considering both temperature and mass fraction of nanoparticle is proposed:

$$C_{\mathrm{nf}} = a + b\varphi + cT + d\varphi^2 + e\varphi T + fT^2 \tag{12}$$

where *a, b, c, d, e*, and *f* are fitted by the experimental data, and shown in tab. 1, and T [°C] – the temperature.

Table 1. Parameters in eq. (12)

a	*b*	*c*	*d*	*e*	*f*	R^2
3.918	–218.3	0.006596	3.185e+05	5.278	–5.35e-05	0.9837

Figure 9 shows the comparison between the predicted values by the fitted eq. (12) and the experimental data. It indicates that this formula can give a precise prediction and has a very good agreement with the experimental data for wide range of operating temperatures and nanoparticle concentrations. The maximum error is 0.86%, and the R^2 is about 0.983.

Conclusions

A GO+Al_2O_3 water hybrid nanofluid was prepared and its stability was investigated. The specific heat of the hybrid nanofluid was measured at the concentration of 0.05-0.1 5 wt.% and temperature of 20-70 °C. The effects of the nanoparticle mass fraction and temperature on the specific heat capacity of the hybrid nanofluids were studied. Moreover, a fitted formula of the specific heat of the hybrid nanofluid was proposed based on the experimental data. The key results of this work are as follows.

The specific heat capacity of the nanofluid decreases with the increase of nanoparticle mass fraction. The mass fraction of nanoparticle affects the specific heat of hybrid nanofluid more significantly at lower temperature. The specific heat increases with the increase of temperature, which affects the specific heat more significantly than mass fraction of nanoparticle. The maximum drop amplitude of the specific heat reduction ratio of the hybrid nanofluid is up to four times. The specific heat of the hybrid nanofluid is higher than that of single nanoparticle nanofluids, but the differences among the specific heat of nanofluids are not very large, with maximum difference of 1.33% at 20 °C. The traditional models of the specific heat of nanofluids do not predict the specific heat of this hybrid nanofluid, and the fitted formula agrees well with the experimental data, taking into account the effects of mass fraction of the hybrid nanoparticle and temperature simultaneously.

Acknowledgment

This study is supported by National Natural Science Foundation of China (51306060), Key Research and Development and Promotion Project in Henan province - Science and Technology (International Cooperation) (182102410087), Innovative Research Team (in Science and Technology) in University of Henan Province (19IRTSTHN011), and Special Support Plan for High-level Talents of Henan Province-“ZHONGYUAN Thousand Talent Program”(ZYQR201810075). We would like to thank to anonymous reviewers for the excellent feedback.

Nomenclature

$C_{p,\mathrm{bf}}$ – base solution specific heat capacity, [$\mathrm{Jkg^{-1}K^{-1}}$]
$C_{p,\mathrm{nf}}$ – nanofluids specific heat capacity, [$\mathrm{Jkg^{-1}K^{-1}}$]
M_1 – nanofluid sample of mass, [g]
M_2 – standard sample of mass, [g]
Q_1 – released heat by hybrid nanofluid, [J]
Q_2 – absorbed heat by deionized water, [J]
Q_L – heat loss, [J]
T_1 – nanofluid sample temperature, [°C]
T_2 – standard sample temperature, [°C]
T_3 – the mixing temperature, [°C]
w – mass fraction, [–]

Greek symbols

δ – relative error
ρ – density, [$\mathrm{kgm^{-3}}$]
φ – volume fraction, [–]

References

[1] Hemmat, Esfe, M., Hajmohammad, M. H., Thermal Conductivity and Viscosity Optimization of Nanodiamond-Co_3O_4/EG (40:60) Aqueous Nanofluid Using NSGA-II Coupled with RSM, *Journal of Molecular Liquids*, *238* (2017), July, pp. 545-552
[2] Ganvir, R. B., Walke, P. V., Heat Transfer Characteristics in Nanofluid-A review, *Renewable and Sustainable Energy Reviews*, *75* (2017), Aug., pp. 451-460
[3] Aberoumand, S., Jafarimoghaddam, A., Tungsten (III) Oxide (WO_3) – Silver/Transformer Oil Hybrid Nanofluid: Preparation, Stability, Thermal Conductivity and Dielectric Strength, *Alexandria Engineering Journal*, *57* (2018), 1, pp. 121-130
[4] Aravind, S. S. J., Ramaprabhu, S., Graphene-Multiwalled Carbon Nanotube-Based Nanofluids for Improved Heat Dissipation, *RSC Advances*, *3* (2013), 13, pp. 4199
[5] Sinz, C. K., *et al.*, Numerical Study on Turbulent Force Convective Heat Transfer of Hybrid Nanofluid, Ag/HEG in a Circular Channel with Constant Heat Flux, *Journal of Advanced Research*, *24* (2016), 1, pp. 1-11
[6] Baby, T. T., Ramaprabhu, S., Experimental Investigation of the Thermal Transport Properties of a Carbon Nanohybrid Dispersed Nanofluid, *Nanoscale*, *3* (2011), 5, pp. 2208-2214
[7] Chandran, M. N., *et al.*, Novel Hybrid Nanofluid with Tunable Specific Heat and Thermal Conductivity: Characterization and Performance Assessment for Energy Related Applications, *Energy*, *140* (2017), Dec., pp. 27-39
[8] Ahammed, N., *et al.*, Entropy Generation Analysis of grapheme-alumina Hybrid Nanofluid in Multiport Minichannel Heat Exchanger Coupled with Thermoelectric Cooler, *International Journal of Heat and Mass Transfer*, *103* (2016), Dec., pp. 1084-1097
[9] Gao, Y. G., *et al.*, Measurement and Modeling of Thermal Conductivity of Graphene Nanoplatelet Water and Ethylene Glycol Base Nanofluids, *International Journal of Heat and Mass Transfer*, *123* (2018), Aug., pp. 97-109
[10] Sang, L., Liu, T., The Enhanced Specific Heat Capacity of Ternary Carbonates Nanofluids with Different Nanoparticles, *Solar Energy Materials and Solar Cells*, *169* (2017), Sept., pp. 297-303

[11] Hassan, N., *et al.*, Recent Developments in Phase Change Materials for Energy Storage Applications: A review, *International Journal of Heat and Mass Transfer, 129* (2019), Feb., pp. 491-523
[12] Ranga Babu, J. A., *et al.*, State-of-Art Review on Hybrid Nanofluids, *Renewable and Sustainable Energy Reviews*, *77* (2017), Sept., pp. 551-565
[13] Sundar, S. L., *et al.*, Hybrid Nanofluids Preparation, Thermal Properties, Heat Transfer and Friction Factor – A review, *Renewable & Sustainable Energy Reviews*, *68* (2017), Feb., pp. 185-198
[14] Wang, X. Q., Mujumdar A. S., Heat Transfer Characteristics of Nanofluids: A review, *International Journal of Thermal Sciences*, *46* (2007), 1, pp. 1-19
[15] Yarmand, H., *et al.*, Study of Synthesis, Stability and Thermo-Physical Properties of Graphene Nanoplatelet/Platinum Hybrid Nanofluid, *International Communications in Heat and Mass Transfer*, *77* (2016), Oct., pp. 15-21
[16] Saeedinia, M., *et al.*, Thermal and Rheological Characteristics of CuO-Base Oil Nanofluid Flow Inside a Circular Tube, *International Communications in Heat and Mass Transfer*, *39* (2012), 1, pp. 152-159
[17] Liu, Y. S., Yang, Y. Z., Investigation of Specific Heat and Latent Heat Enhancement in Hydrate Salt Based TiO_2 Nanofluid Phase Change Material, *Applied Thermal Engineering*, *124* (2017), Sept., pp. 533-538
[18] Barbes, B., *et al.*, Thermal Conductivity and Specific Heat Capacity Measurements of Al_2O_3 Nanofluids, *Journal of Thermal Analysis & Calorimetry*, *111* (2012), 2, pp. 1615-1625
[19] Zhou, S. Q., Ni, R., Measurement of the Specific Heat Capacity of Water-Based Al_2O_3 Nanofluid, *Applied Physics Letters*, *92* (2008), 9, 93123
[20] Wu, Y. Y., *et al.*, Effect of Timeliness on the Thermal Properties of Paraffin-Based Al_2O_3 Nanofuids, *Modern Physics Letters B*, *33* (2019), 5, 1950051
[21] Nieh, H. M., *et al.*, Enhanced Heat Dissipation of a Radiator using Oxide Nanocoolant, *International Journal of Thermal Sciences*, *77* (2014), Mar., pp. 252-261
[22] Vajjha, R. S., Das, D. K., Specific Heat Measurement of Three Nanofluids and Development of New Correlations, *J. Heat Transfer*, *131* (2009), 7, pp. 071601-071607
[23] Ho, C. J., *et al.*, Preparation and Properties of Hybrid Water-Based Suspension of Al_2O_3 Nanoparticles and MEPCM Particles as Functional Forced Convection Fluid, *International Communications in Heat and Mass Transfer*, *37* (2010), 5, pp. 490-494
[24] Hu, Y. W., *et al.*, Enhanced Heat Capacity of Binary Nitrate Eutectic Salt-Silica Nanofluid for Solar Energy Storage, *Solar Energy Materials and Solar Cells*, *192* (2019), Apr., pp. 94-102
[25] Kauffeld, M., Gund, S., Ice Slurry-History, Current Technologies and Future Developments, *International Journal of Refrigeration*, *99* (2019), Mar., pp. 264-271
[26] Liu, Y. D., *et al.*, Nucleation Mechanism of Nanofluid Drops under Acoustic Levitation, *Applied Thermal Engineering*, *130* (2018), Feb., pp. 40-48
[27] Liu, Y. D., *et al.*, Nucleation Rate and Supercooling Degree of Water-Based Graphene Oxide Nanofluids, *Applied Thermal Engineering*, *115* (2017), Mar., pp. 1226-1236
[28] Liu, Y. D., *et al.*, Containerless Nucleation Behavior and Supercooling Degree of Acoustically Levitated Graphene Oxide Nanofluid PCM, *International Journal of Refrigeration*, *60* (2015), Dec., pp. 70-80
[29] Ijam, A., *et al.*, Stability, Thermo-Physical Properties, and Electrical Conductivity of Graphene Oxide-Deionized Water/Ethylene Glycol Based Nanofluid, *International Journal of Heat and Mass Transfer*, *87* (2015), Aug., pp. 92-103
[30] Zhang, H. Y., *et al.*, Stability, Thermal Conductivity, and Rheological Properties of Controlled Reduced Graphene Oxide Dispersed Nanofluids, *Applied Thermal Engineering*, *119* (2017), June, pp. 132-139
[31] Kumar, N., *et al.*, Experimental Study of Thermal Conductivity, Heat Transfer and Friction Factor of Al_2O_3 Based Nanofluid, *International Communications in Heat and Mass Transfer*, *90* (2018), Jan., pp. 1-10
[32] Xie, Y., *et al.*, The Effect of Novel Synthetic Methods and Parameters Control on Morphology of NanoAlumina Particles, *Nanoscale Research Letters*, *11* (2016), 1, pp. 259
[33] Haque, A. K. M. M, *et al.*, Forced Convective Heat Transfer of Aqueous Al_2O_3 Nanofluid Through Shell and Tube Heat Exchanger, *J. Nanosci Nanotechnol*, *18* (2018), 3, pp. 1730-1740
[34] Charab, A. A., *et al.*, Thermal Conductivity of Al_2O_3 + TiO_2/Water Nanofluid: Model Development and Experimental Validation, *Applied Thermal Engineering*, *119* (2017), June, pp. 42-51
[35] Muhammad, A., *et al.*, Sedimentation and Stabilization of Nanofluids with Dispersant, *Colloids and Surfaces A: Physicochemical and Engineering Aspects*, *554* (2018), Oct., pp. 86-92

[36] Said, Z., *et al.*, Energy and Exergy Analysis of a Flat Plate Solar Collector using Different Sizes of Aluminium Oxide Based Nanofluid, *Journal of cleaner production*, *133* (2016), Oct., pp. 518-530
[37] Pralat, K., Comparison of Electrocalorimetric and Cooling Methods to Determine Specific Heat of Aqueous Solutions of the Sodium Salt Carboxymethylcellulose, *Arab Journal of Science Engineering*, *40* (2015), 12, pp. 34069-3415
[38] Semmar, N., *et al.*, Specific Heat of Carboxymethyl Cellulose and Carbopol Aqueous Solutions, *Termochimica Acta*, *402* (2003), 1-2, pp. 225-235
[39] Semmar, N., *et al.*, Analytical Expressions of Specific Heat Capacities for Aqueous Solutions of CMC and CPE, *Termochimica Acta, 419* (2004), 1-2, pp. 51-58
[40] Ramaswamy, H. S., Zareifard, M. R., Evaluation of Factors Influencing Tube-Flow Fluid-to-Particle Heat Transfer Coefficient using a Calorimetric Technique, *Journal of Food Engineering*. *45* (2000), 3, pp. 127-138
[41] Villano, P., *et al.,* Specific Heat Capacity of Lithium Polymer Battery Components, *Termochimica Acta*, *402* (2003), 1-2, pp. 219-224
[42] Stoliarov, S. I., Walters, R. N., Determination of the Heats of Gasification of Polymers using Differential Scanning cAlorimetry, *Polymer Degradation and Stability*, *93* (2008), 2, pp. 422-427
[43] Kato, H., Sasaki, K., Avoiding Error of Determining the Martensite Finish Temperature Due to Thermal Inertia in Differential Scanning Calorimetry: Model and Experiment of Ni–Ti and Cu–Al–Ni Shape Memory Alloys, *Journal of Material Science*, *47* (2012), 3, pp. 1399-1410
[44] Kwarciak, J., Morawiec, H., Some Interpretation Problems of Thermal Studies of the Reversible Martensitic Transformation, *Journal of Material Science*, *23* (1988), 2, pp. 551-557
[45] Milkereita, B., *et al.,* Precipitation Kinetics of an Aluminium Alloy During Newtonian Cooling Simulated in a Differential Scanning Calorimeter, *Termochimica Acta*, *522* (2011), 1-2, pp. 86-95
[46] Kempen, A. T. W., *et al.*, Calibration and Desmearing of Differential Thermal Analysis Measurement Signal Upon Heating and Cooling, *Termochimica Acta*, *383* (2002), 1-2, 2130
[47] Perry, J. H., Chilton, C. H., *Chemical Engineers' Handbook*. McGraw Hill, New York, USA, 1973
[48] Xuan, Y. M., Li, Q., *Theory and Application of Energy Transfer in Nanofluids* (in Chinese), Science Press, Beijing, China, 2010
[49] Sundar, L. S., *et al.*, Enhanced Heat Transfer and Friction Factor of MWCNT-Fe_3O_4/Water Hybrid Nanofluids, *International Communications in Heat & Mass Transfer*, *52* (2014), Mar., pp. 73-83
[50] Ghozatloo, A., *et al.*, Convective Heat Transfer Enhancement of Graphene Nanofluids in Shell and Tube Heat Exchanger, *Experimental Thermal and Fluid Science*, *53* (2014), Feb., pp. 136-141
[51] Altohamy, A. A., *et al.*, Effect of Water Based Al_2O_3 Nanoparticle PCM on Cool Storage Performance, *Applied Thermal Engineering*, *84* (2015), June, pp. 331-338

Paper submitted: April 4, 2019
Paper revised: September 13, 2019
Paper accepted: September 18, 2019
© 2021 Society of Thermal Engineers of Serbia.
Published by the Vinča Institute of Nuclear Sciences, Belgrade, Serbia.
This is an open access article distributed under the CC BY-NC-ND 4.0 terms and conditions.